

Article

SWCNTs/PEDOT: PSS Coated Cotton for Wearable Clothes and Supercapacitor Applications

Nujud Mohammad Badawi ¹, Khalid Mujasam Batoo ^{2,*}, S. Ramesh ¹, K. Ramesh ¹  and Ahamad Imran ²

¹ Centre for Ionics University Malaya, Department of Physics, Faculty of Science, Universiti Malaya, Kuala Lumpur 50603, Malaysia

² King Abdullah Institute for Nanotechnology, King Saud University, P.O. Box-2455, Riyadh 11451, Saudi Arabia

* Correspondence: kbatoo@ksu.edu.sa

Abstract: Herein, we report single-wall carbon nanotubes (SWCNT)/poly(3,4-ethylenedioxythiophene) polystyrene sulfonate (PEDOT: PSS) loading on the transparency and conductivity of pure cotton and systematically studied using a four-probe stack made of copper (Cu) which showed a surface resistance of 0.08 Ω /cm. Moreover, the treated cotton cloth retained its maximum resistance even after three months. Surface morphology was investigated by scanning electron microscopy (SEM) and elemental structure analysis was performed by energy-dispersive X-ray (EDX), while the structural analysis was performed using Fourier transform infrared spectroscopy (FTIR) and X-ray diffraction (XRD) techniques, confirming that there is a good dispersion of SWCNTs/PEDOT: PSS in the cotton sample. The composite cotton/hydrogel polymer/composite cotton achieved a specific capacitance of 212.16 F/g at 50 mV/s. Thermal properties were also investigated using thermogravimetric analysis (TGA) and differential scale calorimetry (DSC). The low surface resistance and thermal stability show that cotton fabric can be a promising candidate for smart wearable textiles and modern circuitry applications.

Keywords: SWCNTs; PEDOT: PSS; resistance; conductive cotton; cotton fabric; smart wearable textile



check for updates

Citation: Badawi, N.M.; Batoo, K.M.; Ramesh, S.; Ramesh, K.; Imran, A. SWCNTs/PEDOT: PSS Coated Cotton for Wearable Clothes and Supercapacitor Applications. *Sustainability* **2023**, *15*, 889. <https://doi.org/10.3390/su15010889>

Academic Editor: Changhyun Roh

Received: 29 November 2022

Revised: 21 December 2022

Accepted: 23 December 2022

Published: 3 January 2023



Copyright: © 2023 by the authors. Licensee MDPI, Basel, Switzerland. This article is an open access article distributed under the terms and conditions of the Creative Commons Attribution (CC BY) license (<https://creativecommons.org/licenses/by/4.0/>).

1. Introduction

Smart wearable devices can be produced using flexible materials in the field of energy, electronics, sensing, and healthcare products. These devices are prepared by incorporating conductive nanostructures single-wall carbon nanotubes and multiwall carbon nanotubes (SWCNTs and MWCNTs) and polymeric nanocomposites (PEDOT: PSS) on the surface of flexible cotton. Smart conductive fabric is an active area of research nowadays due to its growing applications in flexible electronics, wearable devices, and electronic sensors [1]. The fusion of cotton with conductive fillers makes composite cotton with exciting new properties, such as pressure and fatigue sensors [2].

We treated pure cotton using a mixture of SWCNTs and PEDOT: PSS with the addition of dimethyl sulfoxide (DMSO) as a catalyst to make the electrode and using the hydrogel as an electrolyte [3]. As an electrode, composite cotton can be used to incubate nanostructured energy materials such as SWCNTs and PEDOT: PSS. In order to convert pure cotton into conductive cotton, the dipping method is an effective technique. Due to the strong π -bond interaction between SWCNTs and PEDOT: PSS, the π -orbitals overlap to form “ π -bonds” due to SWCNTs being a good conductor and due to the non-positional electrons in the π -orbitals [4]. SWCNTs are formed through graphene-like sp^2 hybridization. These bonds are stronger than the sp^3 bonds found in diamonds and SWCNTs nanotubes are distinguished by their unique strength [5].

The carbon atoms are bonded together through a C–C conduction, where the energy difference between the 2s and 2p orbitals is less than the energy gain. To form the primary structure, the orbitals can fuse in hybrid orbitals, where each carbon atom is bonded to four

carbon neighbors [6]. The hexagonal lattice is the main step in the fusing of single-walled nanotubes with pure cotton and PEDOT: PSS (Figure 1). Additionally, PEDOT: PSS reduces the aggregation of SWCNTs and thus increases the ion pathways and significantly improves the electron transfer efficiency in cotton [6].

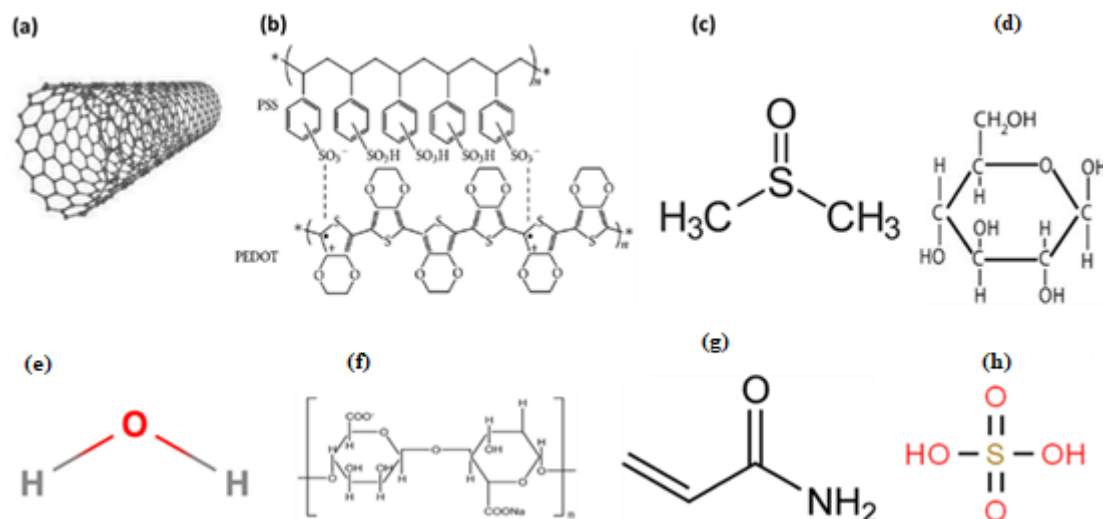


Figure 1. The chemical structures of (a) SWCNTs, (b) PEDOT: PSS, (c) DMSO, (d) cotton, (e) DI, (f) Na-Alginate, (g) AAM and (h) H_2SO_4 .

The key to flexible collapsible electrodes is to achieve flexibility and increase their service life under repeated cyclic loading with certain stress. Extensibility refers to the ability of stretchable flexible electrodes to maintain electrical conductivity under mechanical deformation. In the field of supercapacitors, this is a research hotspot for preparing materials with more flexibility and even extensibility. In mechanics, cotton is a good way to achieve overall structural expansion. In addressing the presence of carbonaceous materials, an easy and inexpensive preparation process that is compatible with various new materials is a necessary step to achieve large-scale preparation. For charge storage mechanisms, supercapacitors (SCs) are classified as double-layer electrolytic capacitors (EDLCs) and pseudo-capacitors (PCs). It can contain EDLCs, activated carbon, graphene derivatives, carbon nanotubes, carbon fabrics, etc., as electromagnetic materials (EMs), while computers usually use conductive polymers such as polyaniline, polypyrrole, polythiophene, polythiophene derivatives, etc., transition metal oxides, and transition metal nitrides, carbides, and sulfides. Supercapacitors (SCs) have many advantages such as long cycle life, high energy density, and low maintenance cost [7]. On the other hand, hydrogels have attracted the attention of researchers in the field of energy storage systems, given that they are multiple building blocks for the multiple uses of life. Hydrogels are interlocking 3D hydrated mesh materials based on hydrophilic mechanical elasticity, reversibility, and tunability. Thus, the complexities and diversity found in hydrogels populate various energy storage devices that can be bent, stretched, compressed, as well as deformed into arbitrary different shapes [3].

In this work, the conductive cotton fabric has been prepared by the dip-coating method of SWCNTs/PEDOT: PSS which was treated in the presence of dimethyl sulfoxide (DMSO) to destabilize the ripple of the cotton fibers, allowing better incorporation of SWCNTs and cotton fibers, followed by heating for 1 h at $100\text{ }^\circ\text{C}$. SEM, EDX, XRD, FTIR, and TGA were used to characterize the SWCNTs/PEDOT: PSS coated cotton. The conductivity of the materials was determined using a four-line probe method. The conductivity of the treated cotton fabric was monitored for three months. A low-cost, highly flexible, and scalable supercapacitor was assembled from a highly conductive stretchy composite cotton. By incorporating cotton-based high-conducting single-walled carbon nanotubes (SWCNTs) and PEDOT: PSS into the polymer hydrogel, we demonstrate that the capacitor has high capacity, is flexible, and is based on environmentally friendly materials. Electrochemical

studies were carried out using a sandwich natural polymer hydrogel as an electrolyte between SWCNTs/PEDOT: PSS coated replica cotton electrodes.

2. Materials and Methods

2.1. Chemicals and Materials

A single-wall carbon nanotube (SWCNTs), with an individual diameter $\sim 1.8 \pm 0.3$ nm, an individual length $> 5 \mu\text{m}$, carbon purity $> 98\%$, and BET surface area $\sim 500 \text{ m}^2/\text{g}$ was purchased with an initial flake size of 100 mesh from Sigma-Aldrich (308068-56-6). Poly (3,4 methylenedioxy thiophene and poly (4-styrene sulfonate) (PEDOT: PSS) (483095-250G), along with dimethyl sulfoxide (DMSO) (assay 99.9%), was also purchased from Sigma-Aldrich (67-68-5). Pure cotton fabric with a weight of 100 g m^{-2} was purchased from Egypt. Deionized water (DI) was used as a solvent, while sodium alginate ($\text{NaC}_6\text{H}_7\text{O}_6$) (Na-Alginate) (SA, chemically pure) (9005-38-3), Acrylamide (AAM) (79-06-1), and Sulfuric Acid (H_2SO_4) (7664-93-9) to prepare the hydrogel was purchased from Sigma-Aldrich. The chemical structure of all the materials used is shown in Figure 1.

2.2. SWCNTs/PEDOT:PSS Ink Fabrication

A total of 0.5 mL of DMSO was dissolved in deionized water with help and then sonicated. An amount of 1.6 mg/mL concentration of SWNTs was then dispersed in the solution and sonicated for 5 min. A total of 5 mL PEDOT: PSS was then added to the solution as shown in Schematic Figure 2.

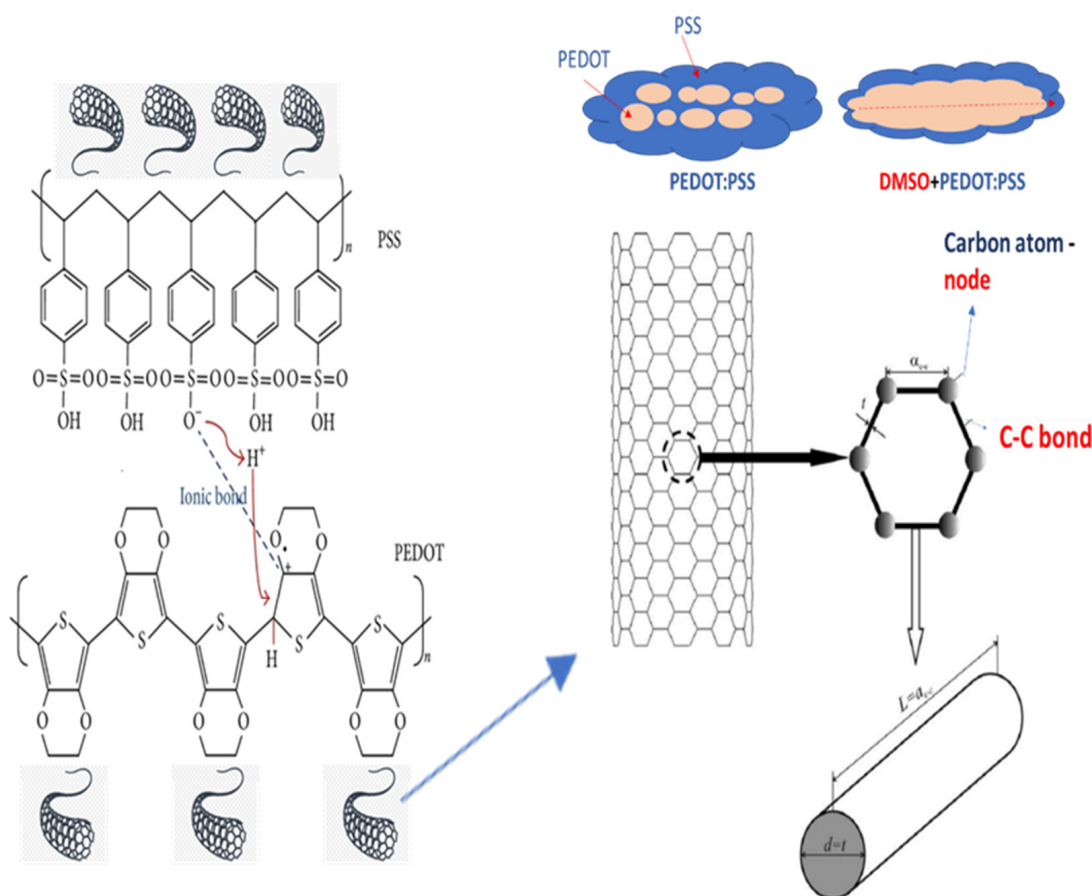


Figure 2. Proposed mechanism of synthesized composite SWCNTs/PEDOT: PSS ink.

2.3. SWCNTs/PEDOT: PSS Cotton Preparation Procedure

Pure cotton $\sim 1\text{--}2$ mm thick was dipped in ink solution of SWCNT/PEDOT: PSS. Due to the high porosity and strong absorbency of cotton, the solution covers cotton quickly.

The SWCNTs/PEDOT: PSS ink composite cotton was dried at 100 °C for an hour to remove the water.

2.4. Poly(acrylamide)/Na-Alginate

Next, 2 gm Na-alginate/100 mL water solution was added with heating and the solution was stirred continuously on a magnetic stirrer at 50° C, and then 7 g of Acrylamide (AAM) monomer was added to the solution. To initiate the polymerization reaction, 0.2 mL solution of H₂SO₄ was added to the solution and was shifted onto a plate. The polymerization reaction was completed after 24 h. The final product was heat-treated for 1 h to remove any water content (Figure 3).

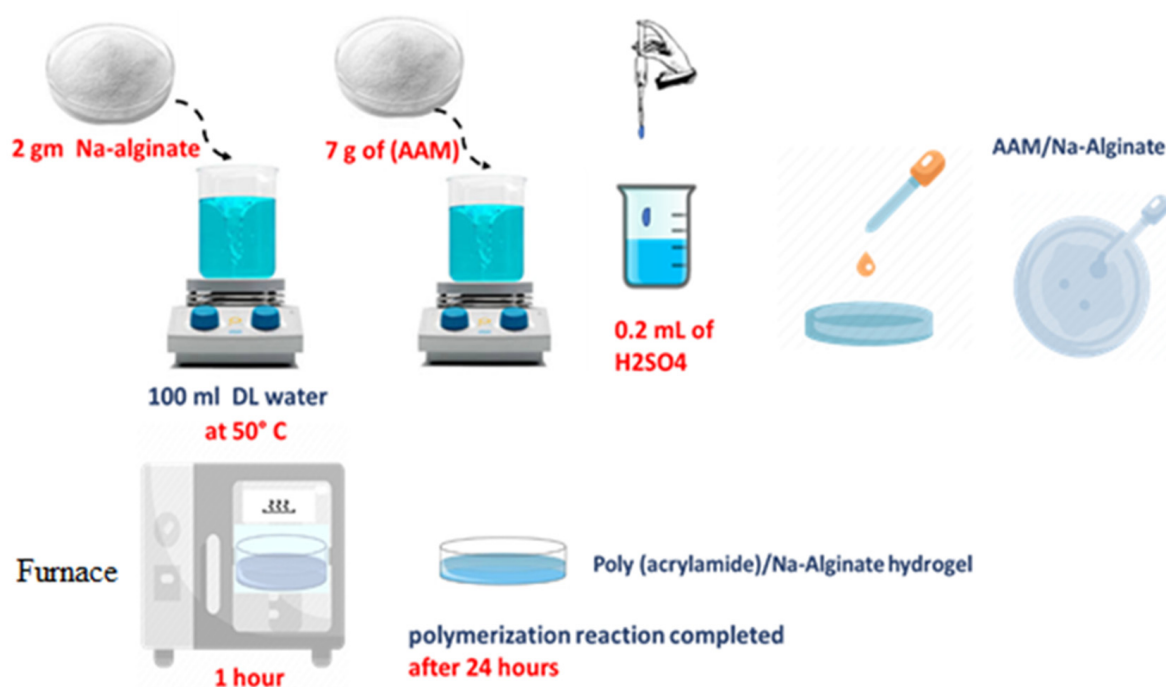


Figure 3. Preparation of Poly(acrylamide)/Na-Alginate hydrogel electrolyte.

2.5. Synthesis of Hydrogel Electrolytes

Poly(acrylamide)/Na-Alginate hydrogel electrolytes were developed by the free radical method. It is a fast and error-free method. The polymerization process was carried out in stages. In the first stage, the hydrogel formed free radicals when exposed to heat by heating. These free radicals generated more free radicals on the backbone of Poly(acrylamide) and Na-Alginate. Long-chain polymers were formed in the second stage after drying the sample in the oven through a hydrogel network Poly(acrylamide)/Na-Alginate via hydrogen bonding. Finally, by H₂SO₄, the polymer chain is physically bonded to form a stable 3D network. The hydrogel has good water absorption capacity due to hydrophilic amide groups and has good strength. The hydrophilic nature is due to the -OH and -COOH groups. The hydrogels were manufactured by adding different contents of Na-Alginate and Acrylamide to reach the desired equilibrium. The formation of the double lattice hydrogel through the cross-linking chains resulted from the repulsion of the negatively charged COO⁻ groups on the linear AAM chain in the networks which led to the expansion of the lattice structure and the increase in the swell of deionized water. Figure 4 illustrates the mechanism of synthesis of the Poly(acrylamide)/Na-Alginate synthesized electrolyte hydrogel.

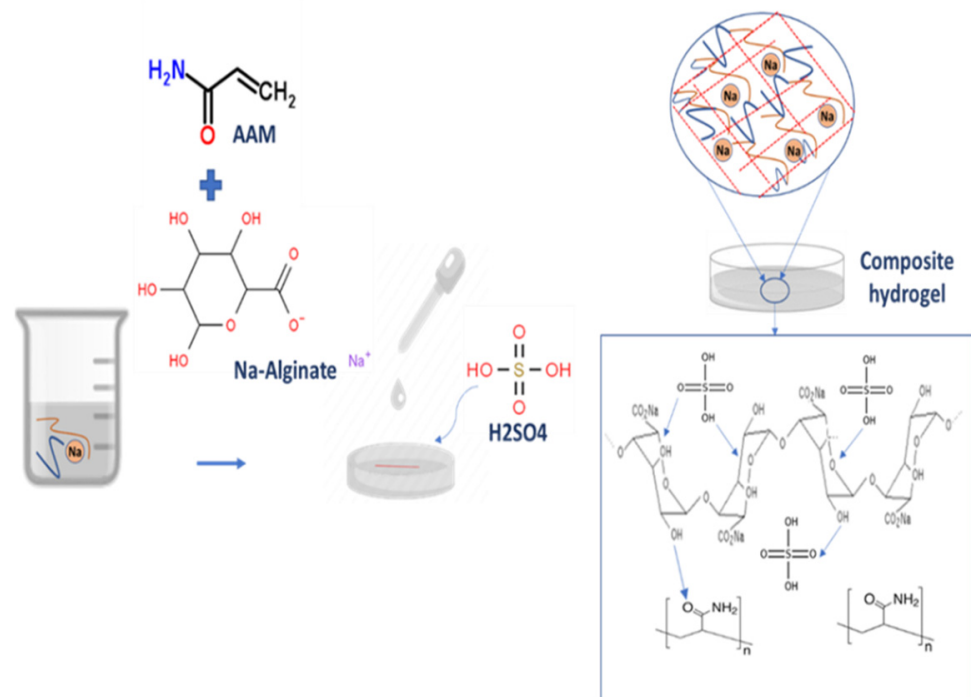


Figure 4. Synthesis of composite hydrogel electrolytes.

3. Characterization and Measurement

The surface morphology of pure and composite cotton was studied using scanning electron microscopy (SEM, Quanta FEG 450) at an accelerating voltage of 5 kV. The samples were coated with gold before SEM analysis. Moreover, energy-dispersive X-ray spectroscopy (EDX) was performed to investigate the elemental composition of pure and composite cotton. In addition, Fourier transformation infrared spectroscopy (FTIR) and X-ray diffraction (XRD) analyses were performed to study the structure and molecular bond formation. XRD patterns were recorded using Cu K α radiation (1.5406 Å) at a current of 30 mA and voltage of 40 kV. Thermogravimetric analysis (TGA) was performed on pure and composite cotton with TGA 1000 instruments, where samples were heated under nitrogen purification from 25 °C to 600 °C at a heating rate of 10 °C/min. The sheet resistance of the composite cotton was measured using a four-line probe technique. To examine the electrical properties of conductive cotton, the electrical resistance of the samples was calculated from the I–V curves at 25 °C having 65% relative humidity [8]. The electrical resistance of conductive cotton was calculated from the formula:

$$R_s = R (w/d) \quad (1)$$

where R is the resistivity, R_s is the bulk resistivity of the fabric, w is the width of the sample (2.5 cm), and d is the distance between the leads (0.35 cm) [9].

The cotton composed by SWCNTs/PEDOT: PSS has high electrical and mechanical capabilities, so the composite cotton can be used as an electrode in supercapacitors. Conductive composite cotton has been used in electrical circuits to light a light-emitting diode (LED) as a supercapacitor.

3.1. Electrochemical Impedance Spectroscopy (EIS) Studies

The ionic conductivity of the composite cotton and the hydrogel was measured using a Hioki 3532-50 LCR HiTESTER impedance spectroscopy over a frequency range of 10 to 10⁶ Hz at a temperature of 25 °C. For this, the samples were kept in the sample holder. This holder is fitted with stainless steel electrodes as a blocking electrode [6]. Bulk resistance was measured from the complex impedance cut-off of the hydrogel electrolyte. The ionic

conductivity (σ) of the supercapacitor was calculated from the measured area of the stapled electrodes [A (cm^2)]. The mass resistance of the supercapacitor of the composite was studied according to the equation [10]:

$$\rho = R \frac{A}{l} \quad (2)$$

3.2. Symmetric Supercapacitor Cell Fabrication and Supercapacitor Performance Studies

The composite cotton-based symmetric supercapacitor cell was fabricated by sandwiching the hydrogel electrolytes between the electron-coated SWCNTs/PEDOT:PSS and the cells were subjected to CV and GCD with the interface of the Gamry 1000 potentiostat [11]. CV measurements were performed at a scanning rate of 20, 30, 40, 60, 70, 80, 90, and 100 mV/sec in the 0–1 V potential window. The specific capacitance (C_{sp}) of EDLC was calculated from CV and GCD measurements using the following equation [12,13]:

$$C_{sp} = \frac{I \Delta t}{m \Delta V} \quad (3)$$

where the symbols C_{sp} , I , t , m , and V represent the specific capacitance, I is current, t is the discharge current, m is the mass of the material, and V is the voltage, respectively.

The relationship of supercapacitor capacitance to the surface area is theoretically expressed by using the following equation [14]:

$$\frac{\epsilon}{4\pi\delta} = \frac{C}{A} \quad (4)$$

where C is the capacitance, A is the surface area of the electrode, ϵ is the dielectric constant of the electrolyte, and δ is the distance from the surface of the electrode to the center of the ionic layer [15,16].

4. Results and Discussion

4.1. Morphology Study

Bio-dispersive X-ray spectroscopy characterization was performed using field-emission scanning electron microscopy (SEM) because it provides detailed information about the morphology of the composite cotton. The internal shape of the hydrogels was carried out on pure cotton and composite cotton from SWCNT/PEDOT: PSS treated. The shape of the lyophilized hydrogel and the hydrogel electrolyte were investigated through a scanning electron microscope (SEM). The scanning electron microscopy images indicate that pure cotton fibers have a smoother surface as shown in Figure 5A(a–c), while the micrographs show cotton fiber samples covered with SWCNTs/PEDOT: PSS as seen in Figure 5A(d–f). The carbon nanotubes are quite visible in the coating and are randomly scattered on the surface of the cotton fibers. These nanotubes are interconnected to each other and frame a thick system that allows for an exchange of current transmission along the surface. FESEM pictures exhibited that SWCNT/PEDOT: PSS was effectively covered on the surface of the cotton [16–19]. Transmission electron microscopy (TEM) at an accelerating voltage of 200 kV was used to examine the powdery SWCNTs. Figure 6a–d shows single-walled carbon nanotubes as a bundle. Single-walled carbon nanotubes (SWCNTs) are conceptually characterized as a cylinder resting on a rolled graphene sheet. It is divided into one well (Figure 6e).

The elemental purity of the samples was verified through EDX measurement. The cotton samples displayed peaks at 0.277 kV and 0.525 kV, respectively, showing the presence of carbon and oxygen as shown in Figure 7. From Figure 7, the EDX estimates for composite cotton shows the presence of sulfur as evidenced by the presence of a peak at 2.307 kV which is a component of DMSO.

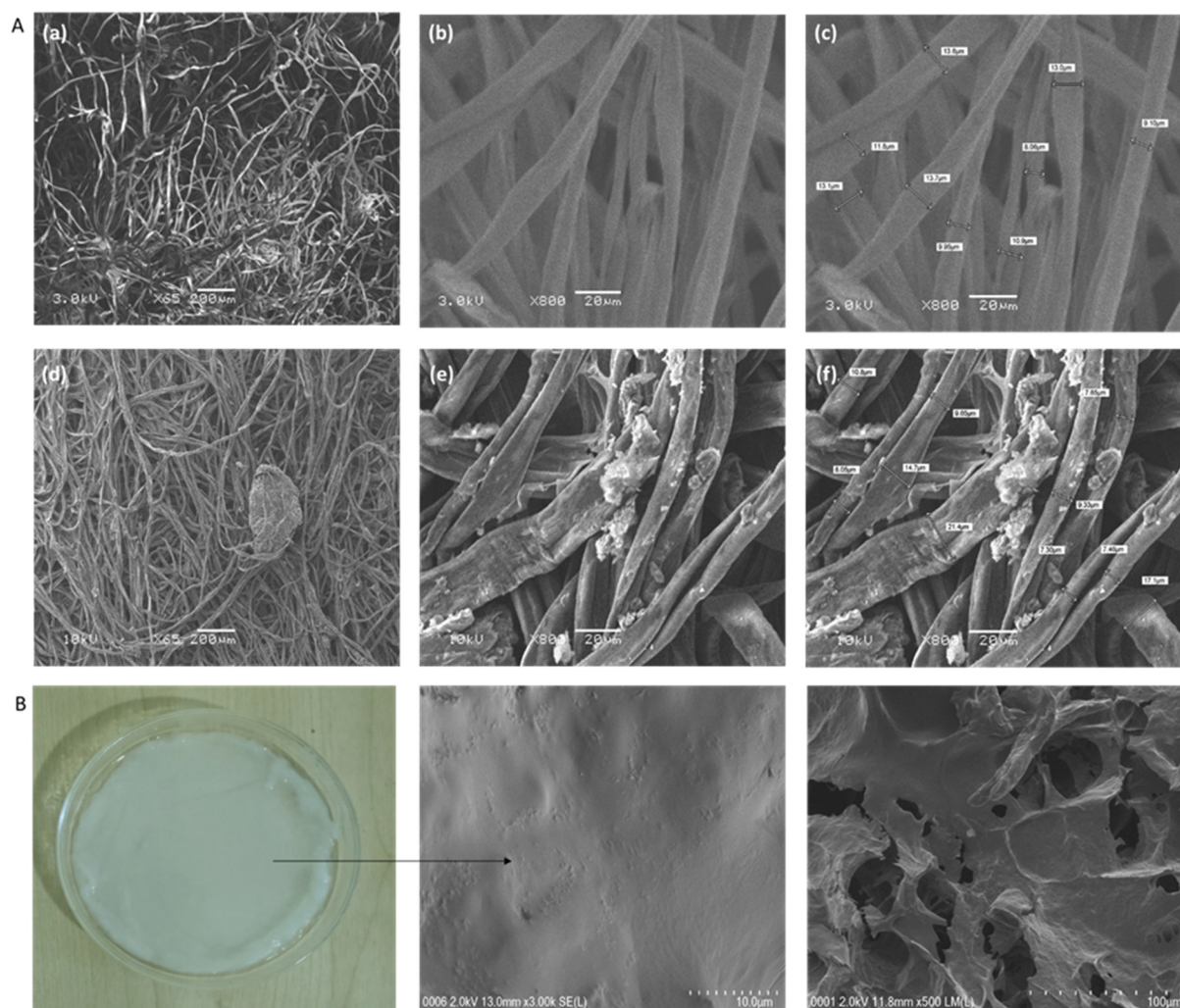


Figure 5. FESEM images: (A) (a,b) original cotton microfibers, (d,e) the conductive microfibers concentrations of SWCNT/PEDOT: PSS, and (c,f) FESEM images showing the cross-section of pure and conductive microfibers at different concentrations of SWCNT/PEDOT: PSS, respectively. (B) Surface morphology images of the hydrogel.

Figure 5B shows the SEM morphology of the hydrogel, where it is seen that the hydrogel exhibited a highly porous three-dimensional network in a regular structure with uniform distribution. The large and uniform pore size is due to the successful formation of a three-dimensional network interconnected with the monomer as well as due to the result of heating the mixture at a constant rate. This highly interconnected network can ensure a large amount of water content [14]. It can be seen that the addition of H_2SO_4 enhanced the density of the polymer network by connecting the pores through the reaction polymerization [20].

4.2. X-ray Diffraction (XRD)

The structural and phase formation of the samples was studied using the X-ray diffraction method. The X-ray diffraction of pure cotton and SWCNT/PEDOT: PSS composite cotton is shown in Figure 8. It can be seen from the XRD pattern that four noteworthy peaks at the angular positions $2\theta = 18^\circ, 22.6^\circ, 36.2^\circ,$ and 38° are observed. The peaks are indexed to the Miller indices (110), (002), (040), and (211) and are ascribed to the spectral reflections generated by pure cotton. Pure represents the structure of the main component of cotton cellulose as seen in Figure 8a [21]. Moreover, the XRD pattern of the composite cotton reveals the higher intensity patterns at the angular positions $2\theta = 22^\circ$ and 25.8° ,

which are indexed as (222) and (120) and represent the characteristic peaks corresponding to the SWCNTs/PEDOT: PSS.

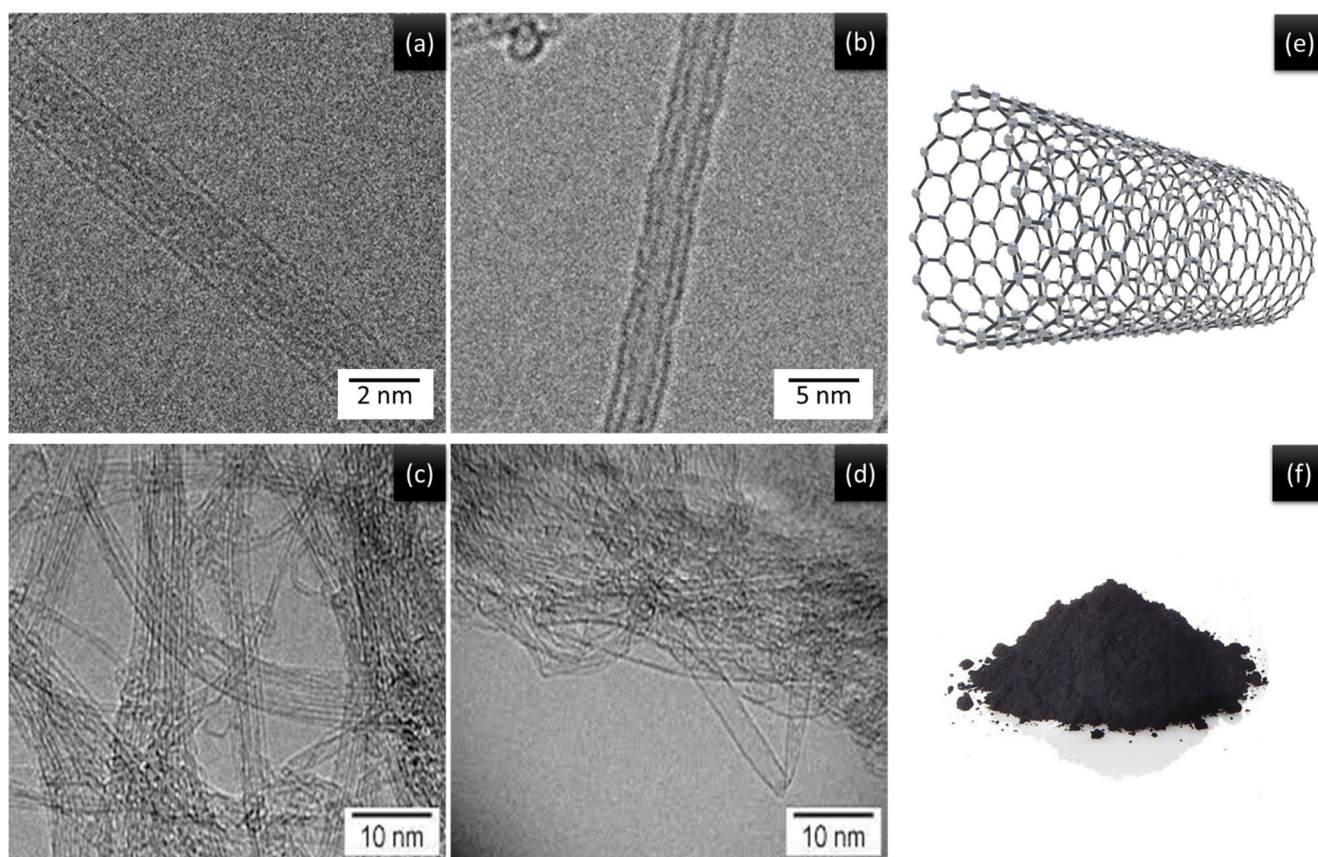


Figure 6. (a–d) TEM images of SWCNT. (e) Schematic diagrams of SWCNT. (f) SWCNT powder.

It was observed that the spectra of all samples, especially the cellulose-based ones, showed some peaks in the region, which are ascribed due to the structural bending, glycoside binding, and ring deformation of C–O–H, C–C–H, C–O, C–C, and C–O–C groups in cellulose and hemicellulose [22–24]. The peak observed around 37.5 in the cotton samples is related to the crystallization of cellulose (C–C, C–O, and C–O bonds and ring deformation). Pure cotton shows strongly capped X-ray peaks that confirm the high stereoscopic organization of its fragments while the X-ray peak of pure cotton testing is essentially more extensive. The peak located around 28° disappeared, which shows the presence of a C=C bond in the composite cotton, and hence confirms the successful composite formation of cotton with SWCNT/PEDOT: PSS as shown in Figure 8b. The SWCNT/PEDOT: PSS composite cotton shows an improvement in the steric regularity of the cellulose network due to the development of hydrogen bonds, which in turn increases the length of the polymer chains. This indicates the good treatment of cotton by dipping it in the solution [25,26].

4.3. Fourier Transform Infrared (FTIR) Spectroscopy

Figure 9 represents the FTIR spectra of pure and synthetic cotton from SWCNTs and PEDOT: PSS. In the spectrum of pure cotton, the peaks at 1300, 1100, and 1058 cm^{-1} were observed which represent the O–H vibration stretching [25,27]. IR bands at 1660 cm^{-1} represent the characteristics of the CH₂ group, while the peaks at 1610 cm^{-1} , 1543 cm^{-1} , 1404 cm^{-1} , and 1240 cm^{-1} , respectively, represent the C=C stretching vibration, the C–H distortion at 750 and 710 cm^{-1} , and the C–O stretching vibration at 1270, 1680, and 810 cm^{-1} . Curve b in Figure 5 represents the composite cotton spectrum having three major peaks at 1230 cm^{-1} , 1185 cm^{-1} , and 1030 cm^{-1} , respectively, that represent the

asymmetric stretching vibration of C–C and the stretching vibration of the O–H group [28].

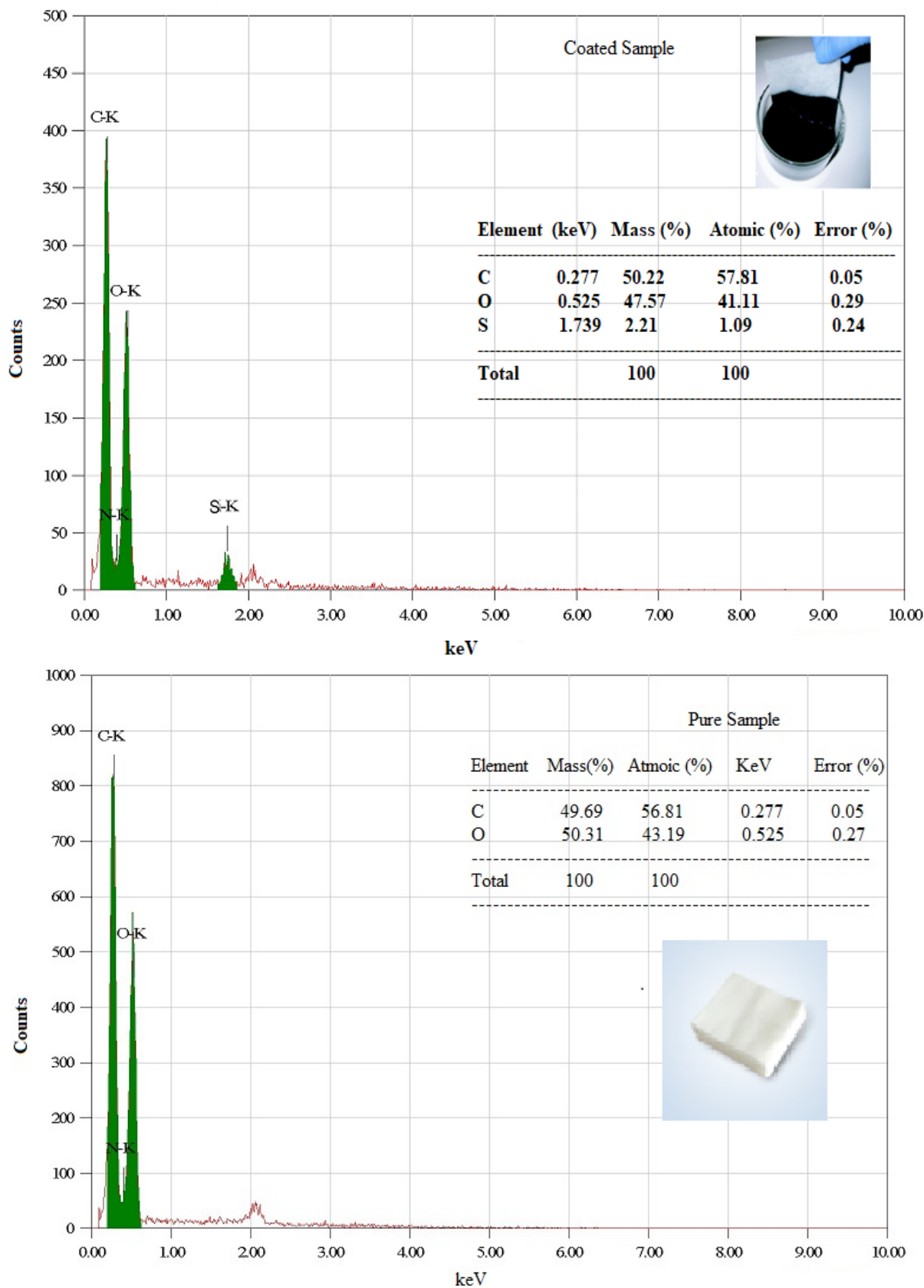


Figure 7. EDX analysis of pure cotton and cotton with SWCNT/PEDOT: PSS.

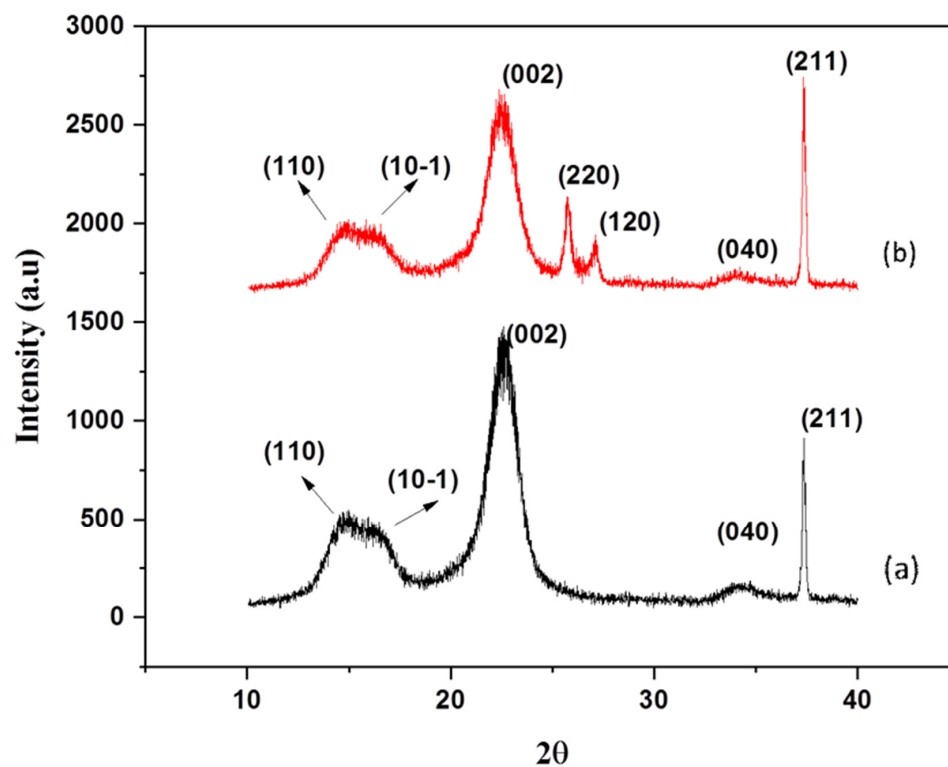


Figure 8. X-ray diffraction of pure cotton fabric (a) and (b) its SWCNT/PEDOT:PSS coated analogs.

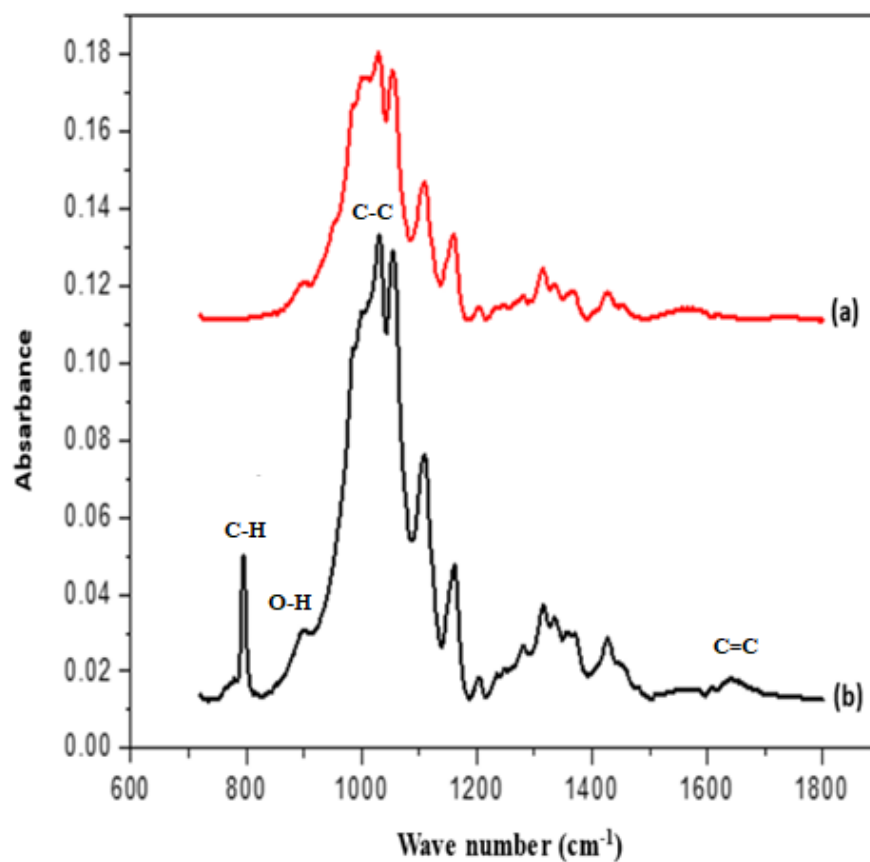


Figure 9. FTIR spectra of (a) pure cotton and (b) composite cotton coated with SWCNT/PEDOT:PSS.

The peaks for composite cotton can be easily observed at 3480 cm^{-1} which represents the O-H stretching vibration and the characteristic peak at 1656 cm^{-1} which represents the C=C bond, with the shift of peak, and with the successful blending of cotton with SWCNT/PEDOT: PSS [29]. Additionally, the composite cotton peak at 790 cm^{-1} represents the C-H and O-H stretching vibration exhibited for composite cotton.

4.4. Thermogravimetric Analysis (TGA)

TGA analysis is an important tool to study the thermal stability and material degradation pattern of pure and SWCNT/PEDOT: PSS coated composite cotton. The thermogravimetric pattern for the prepared samples was performed in the temperature range of $25\text{--}600\text{ }^{\circ}\text{C}$ as shown in Figure 10a,b. The thermal diagram of pure cotton is shown in Figure 10 (a), where we see three phases. The first phase of mass loss occurred in the temperature range of $100\text{--}240\text{ }^{\circ}\text{C}$ which is due to the presence of bound moisture and water molecules. The second phase of weight loss can be seen at $260\text{ }^{\circ}\text{C}$ due to the decomposition of the oxygen-containing functional groups, such as hydroxyl ($-\text{OH}$) and epoxy ($\text{C}-\text{O}-\text{C}$) which turn into molecules of gas (carbon dioxide and water vapor) [21]. The third stage of weight loss can be seen at $400\text{--}600\text{ }^{\circ}\text{C}$. TGA analysis shows the high thermal stability and decomposition of composite cotton. In Figure 10b, the decomposition of the compound cotton shows three stages, with the first stage ranging from $150\text{ to }280\text{ }^{\circ}\text{C}$, where free water is absorbed and mutual irrigation occurs, and the second stage at $372\text{ }^{\circ}\text{C}$, in which the latter can be attributed to the slightly more fibrillation of the cellulose fibers during the reaction (mainly during the ammonia hydrolysis phase), which leads to a higher surface area release rate for the less thermally stable fibers. Thermal decomposition of these materials under flow oxygen can increase the rate of degradation and the third stage ranges from $430\text{ to }600\text{ }^{\circ}\text{C}$ for the combined cotton presumably due to evaporation of decomposed water and decomposition of surface functionalities, weight loss due to the combustion of SWCNTs [30]. The weight loss rate of composite cotton was noted significantly lower than that of pure cotton [15], which is due to the amount of oxygen-containing functional groups of SWCNTs fibers, such as hydroxyl (OH) and epoxy ($\text{C}-\text{O}-\text{C}$) [22].

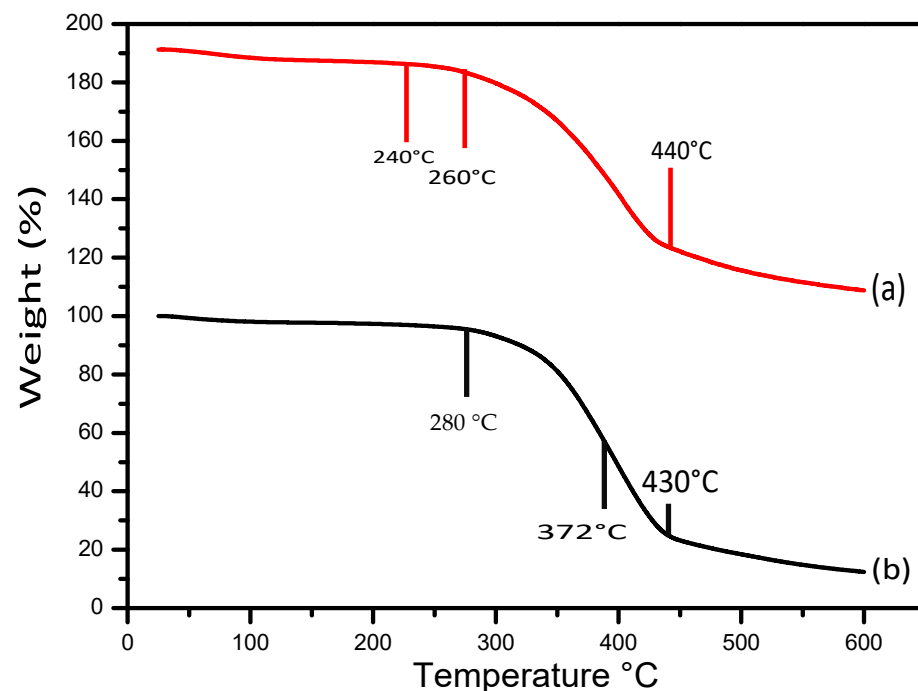


Figure 10. TGA thermograms of pure cotton (a) and (b) SWCNT/PEDOT: PSS coated cotton.

4.5. Electrochemical Impedance Spectroscopy (EIS)

The basic and important property of an electrode and an electrolyte to be used in energy storage devices is ionic conductivity. The ionic conductivity of the composite cotton and the hydrogel was measured by electrochemical impedance spectroscopy. Figure 11 shows a Nyquist diagram of the hydrogel electrolytes and the composite cotton. The Nyquist plot consists of two regions, where the low-frequency region indicates the capacitive characteristics, and the high-frequency region indicates electrical equivalent series resistance (ESR) [31]. A low ESR value is observed due to the rapid transport of charge carriers at the electrolyte interface. Mobile ions are the charge carriers in the system that control the overall electrical conductivity [32]. In these samples, the vertical lines parallel to the imaginary axis at lower frequencies show the internal charge resistance within the electrode and the electrolyte, the resistance of the active material of the composite cotton, the interfacial resistance of electrolyte/hydrogel contact, and the collector current. We observe a straight line vertical to the imaginary axis [33]. Despite this, the hydrogel did not show a straight line perfectly parallel to the imaginal axis [34]. The ionic conductivity, σ (S cm^{-1}), of polymer gel electrolyte was estimated using a HIOKI 3532-50 LCR HiTESTER impedance spectrophotometer at a frequency of 10 to 10^6 Hz [35]. Hydrogel and SWCNT/PEDOT:PSS cotton achieved maximum ionic conductivity of 12.5×10^{-3} and 13.8×10^{-3} S/cm, respectively. A stainless-steel sample holder with electrodes was used for analysis. The bulk resistance was calculated from the slope of the complex impedance plots [36,37]. It is noted from the Cole–Cole plots that the impedance values of the composite cotton are lower than the pure hydrogel. The straight-line values suggest that the impedance values are higher and beyond the measurement frequency range of our instrument [38,39].

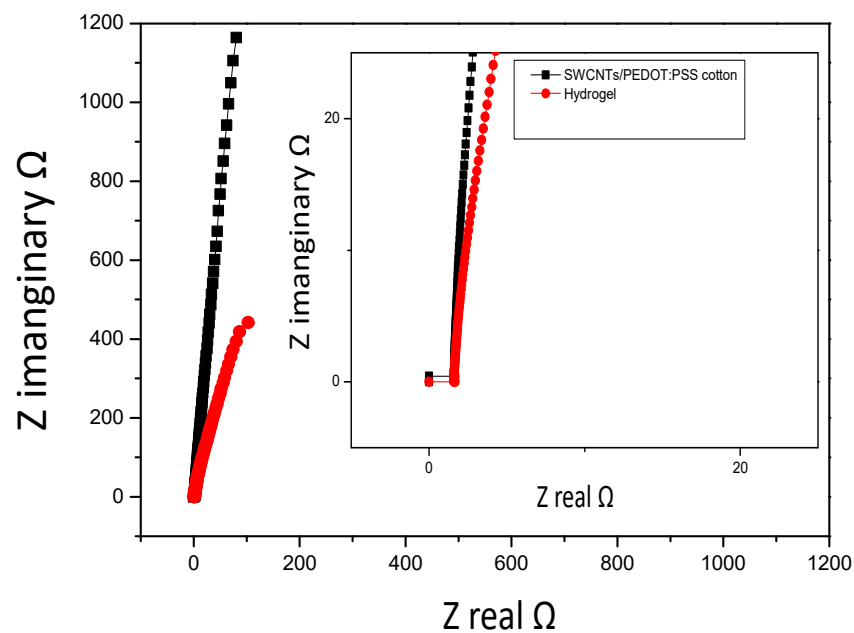


Figure 11. Plot of real vs. imaginary impedance spectroscopy.

4.6. I–V Measurement

A four-line probe method was used to investigate an effective reduction in the composite cotton with SWCNT/PEDOT:PSS and to study the electrical properties of the composite cotton. The sheet resistance is determined by the condition:

$$\sigma = \frac{w}{R \cdot d} \quad (5)$$

where w is the width ($w = 2.5$ cm) and d ($d = 0.35$ cm) is the separation between the lines. In the pure cotton case, the resistance values are infinite, which means no electrical

conductivity is observed or the pure cotton is insulating [40,41]. However, after processing the SWCNT/PEDOT: PSS surface resistance and electrical conductivity, the surface sheet resistance of the composite cotton, $R_s = 0.08 \Omega/\text{cm}$, is obtained and is shown in Figure 12. The reason for the good electrical conductivity of the composite cotton is due to the effective bonding of the amino groups of the cotton with the carboxyl and hydroxyl groups in the SWCNTs [22]. This can also be demonstrated by studying the thermal properties and resistance stability. Moreover, it may be due to the effective chemical bonding between different functional groups of SWCNT/PEDOT: PSS and cotton [21]. The high electrical conductivity of the treated cotton also demonstrates the efficiency of the SWCNT/PEDOT: PSS mixture on pure cotton and the effective use of the solvent DMSO [42]. Table 1 provides details of the sheet resistance of the various composite cotton structures.

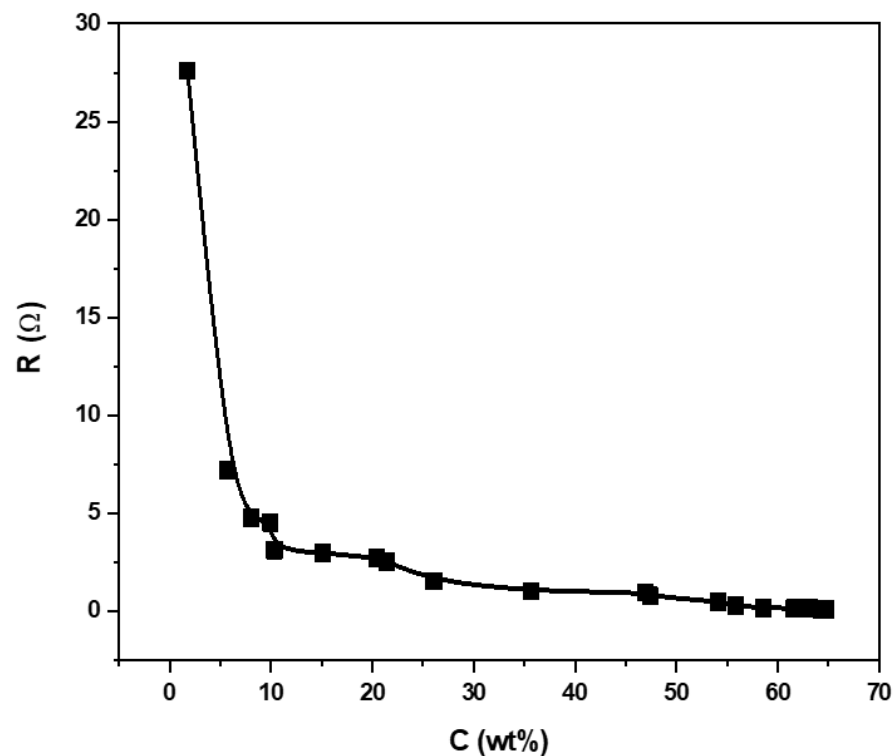


Figure 12. Sheet resistance for pure cotton containing a mixture of SWCNT/PEDOT: PSS.

Table 1. The obtained sheet resistance value is compared with previously published results.

Year	Coated with Material	Sheet Resistance	Material	Reference
2017	Graphene/PEDOT:PSS	25 Ω/Sq . (~1.6S/cm)	Fabric	[43]
2018	PEDOT:PSS	12.1 Ω/Sq .	Cotton	[44]
			spray-Coated	
2017	PEDOT:PSS	1.58 Ω/Sq	Cotton	[45]
	With DMSO		drop-casted	
2013	PEDOT:PSS			
	With (MWCNT)	300–500 Ω/Sq	Film	[46]
2014	(PEDOT:PSS)			
	And hybrid	88 Ω/Sq at a	Film	[47]
2012	SWCNT-PEDOT:PSS	118 Ω/Sq at a	Film	[48]
	-DMSO	transmittance of 90.5%		

4.7. Cyclic Voltammetry (CV)

CV is the most common method to analyze the capacitive behavior of materials in energy storage devices. The electrochemical performance of the cotton-based supercapacitor was measured with the symmetric configuration of the two electrodes where ~3 mm thick hydrogel electrolytes were placed between the electrodes of the composite cotton. CV was studied in the 0–1 V potential range while using a scanning rate between 20 mV/s and 100 mV/s and the CV curves obtained are shown in Figure 13.

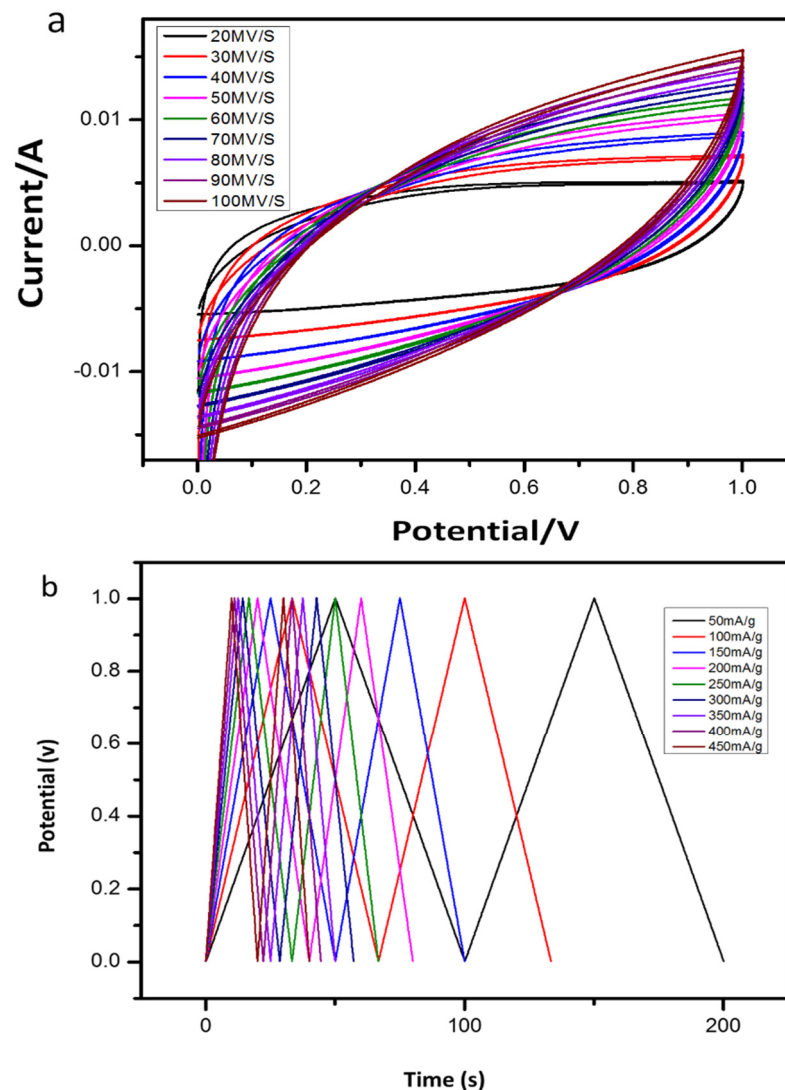


Figure 13. (a) Cyclic voltammetry curves of supercapacitor fabricated by composite cotton and hydrogel. (b) Galvanostatic charge–discharge (GCD) curves of supercapacitor fabricated by composite cotton and hydrogel at different current densities.

The composite cotton-based capacitor exhibited a large CV area and the specific capacitance of 212.16 F/g at 50 mV/s and 310.4 F/g (energy density of 49.57 Wh/kg at a power density of 100.08 W/kg) at 100 mA/g current density compared to AC/NHMA1/AC due to the increase in ionic transport, which is due to the complete dissociation of SWCNT in PEDOT: PSS solution within the synthesized cotton [39–43]. Figure 13b shows the procedure for galvanic charge and discharge analysis at different current densities ranging from 50 to 450 mA/g. All GCD curves for cells were identical, maintaining a high-power triangular shape. Additionally, at a lower current density, the applied current is low, as the EDLC takes a longer time to fully charge and discharge. The diffusion of ions through the electrode material indicates the presence of the active substance. On the other hand, it is

noted that with the increase in the current density, the applied current increases, and the charging and discharging time decreases. The internal resistance produces a lower specific capacitance due to the higher rate of charge transfer.

To achieve the high-power density of the cotton-based capacitor, the exact electrochemical performance of the positive and negative electrodes was tested using charge transportation or matching as shown in Figure 14. The device boasted outstanding electrochemical performance and exhibited a high operating voltage of 9 V, with high durability and flexibility. The proof-of-concept and the obtained results of the electrical conductivity and other properties of the composite cotton showed that the materials can be a promising candidate with great potential in the usage of wearable fabric as mechanical sensors, actuators, and modern circuitry designing [22,44–48], such as electromagnetic shielding, flexible heating elements [42], and capacitor fabric superlative. In addition, the sample was tested before and after the circuit was connected and the supercapacitor was charged several times. It was observed that the electrochemical performance by measuring the periodic voltage before and after connecting the symmetric supercapacitor to the circuit several times did not differ much from before the connection, but rather maintained its shape as shown in Figure 14a.

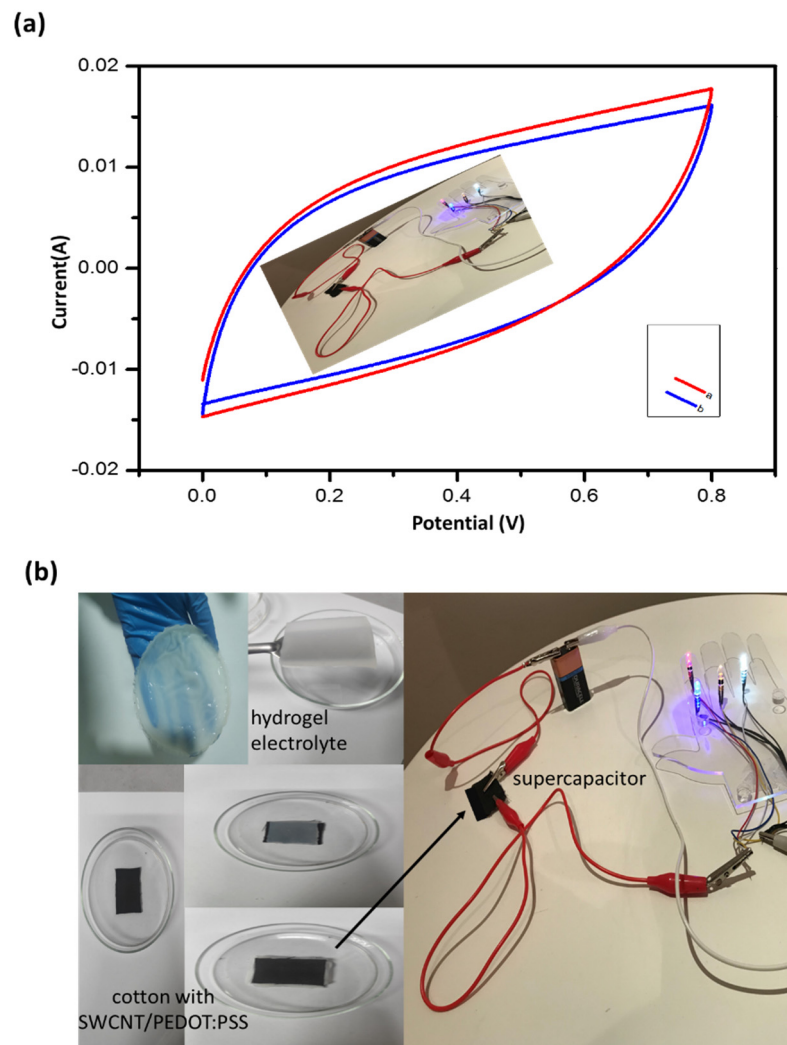


Figure 14. (a) Cyclic voltammety curves of supercapacitor fabricated by composite cotton and hydrogel before and after charging. (b) Set up of device fabrication by connecting two cotton SWCNTs/PEDOT: PSS electrodes with hydrogel as an electrolyte in series.

5. Conclusions

We have successfully grown composite cotton with SWCNT/PEDOT: PSS solution. XRD and FTIR analyses confirmed the formation of the composite structure. The morphology study showed that the 3D porous network structure and initial mapping describe the appropriate dispersion of SWCNT/PEDOT: PSS in pure cotton fibers. Thermal stability and material degradation pattern of pure natural cotton and composite cotton were also studied. TGA analysis and electrochemical impedance analysis also revealed that the presence of SWCNT/PEDOT: PSS in the composite cotton electrode increased the ionic conductivity of the cotton electrode when combined with the polymer hydrogel electrolyte. Using cyclic voltammetry (CV) and galvanic discharge techniques, supercapacitors were fabricated from cotton and polymer hydrogel electrolytes. Electrochemical studies showed that the composite structure exhibits a large CV area and has a specific capacitance of 212.16 F/g at 50 mV/s. The promising electrical properties of the composite materials can be used in wearable electrical fabrics and in designing modern green electrical/electronic circuitry.

Author Contributions: All authors contributed to the study's conception and design. Material preparation, data collection, and analysis were performed by N.M.B. The first draft of the manuscript was written by S.R. and K.R. supervised the experiment, data analysis, and writing of the draft. They both reviewed the first draft and marked their suggestions and comments. K.M.B. reviewed, corrected, and modified the draft and examined the data analysis. All authors have read and agreed to the published version of the manuscript.

Funding: The funding was received by author K. M. Batoo. Deputyship for Research and Innovation "Ministry of Education" in Saudi Arabia funded this work through project number (IFKSURG-2-644).

Institutional Review Board Statement: The authors declare that the research has no human or animal participation.

Informed Consent Statement: Not applicable.

Data Availability Statement: The research data can be provided upon request to the corresponding author.

Acknowledgments: Author K. M. Batoo extends his appreciation to the Deputyship for Research and Innovation "Ministry of Education" in Saudi Arabia for funding this work through project number (IFKSURG-2-644).

Conflicts of Interest: The authors declare they have no competing interest or financial conflict among them.

References

1. Stoppa, M.; Chiolerio, A. Wearable electronics and smart textiles: A critical review. *Sensors* **2014**, *14*, 11957–11992. [[CrossRef](#)] [[PubMed](#)]
2. Hu, X.; Tian, M.; Qu, L.; Zhu, S.; Han, G. Multifunctional cotton fabrics with graphene/polyurethane coatings with far-infrared emission, electrical conductivity, and ultraviolet-blocking properties. *Carbon* **2015**, *95*, 625–633. [[CrossRef](#)]
3. Tadesse, M.; Loghin, C.; Chen, Y.; Wang, L.; Catalin, D.; Nierstrasz, V. Effect of liquid immersion of PEDOT: PSS-coated polyester fabric on surface resistance and wettability. *Smart Mater. Struct.* **2017**, *26*, 065016. [[CrossRef](#)]
4. Lekpittaya, P.; Yanumet, N.; Grady, B.; O'Rear, E.A. Resistivity of conductive polymer-coated fabric. *J. Appl. Polym. Sci.* **2004**, *92*, 2629–2636. [[CrossRef](#)]
5. Terasawa, N.; Asaka, K. Performance enhancement of PEDOT: Poly(4-styrenesulfonate) actuators by using ethylene glycol. *RSC Adv.* **2018**, *8*, 17732–17738. [[CrossRef](#)]
6. Reza, K.; Mabrouk, S.; Qiao, Q. A review on tailoring PEDOT: PSS layer for improved performance of perovskite solar cells. *Proc. Nat. Res. Soc* **2018**, *2*, 02004. [[CrossRef](#)]
7. Mevada, C.; Mukhopadhyay, M. Limitations and recent advances in high mass loading asymmetric supercapacitors based on pseudocapacitive materials. *Ind. Eng. Chem. Res.* **2021**, *60*, 1096–1111. [[CrossRef](#)]
8. Kasprzak, D.; Stepniak, I.; Galiński, M. Electrodes and hydrogel electrolytes based on cellulose: Fabrication and characterization as EDLC components. *J. Solid State Electrochem.* **2018**, *22*, 3035–3047. [[CrossRef](#)]
9. Huang, Y.; Zhong, M.; Huang, Y.; Zhu, M.; Pei, Z.; Wang, Z.; Xue, Q.; Xie, X.; Zhi, C. A self-healable and highly stretchable supercapacitor based on a dual crosslinked polyelectrolyte. *Nat. Commun.* **2015**, *6*, 10310. [[CrossRef](#)]
10. Jin, X.; Sun, G.; Zhang, G.; Yang, H.; Xiao, Y.; Gao, J.; Zhang, Z.; Qu, L. A cross-linked polyacrylamide electrolyte with high ionic conductivity for compressible supercapacitors with wide temperature tolerance. *Nano Res.* **2019**, *12*, 1199–1206. [[CrossRef](#)]

11. Goto, H.; Tomioka, H.; Gunji, T.; Nagao, Y.; Misono, T.; Abe, Y. Preparation of continuous ZrO₂-Y₂O₃ fibers by precursor method using polyzirconoxane. *J. Ceram. Soc. Jpn.* **1993**, *101*, 336–341. [[CrossRef](#)]
12. Meoli, D.; May-Plumlee, T. Interactive electronic textile development: A review of technologies. *J. Text. Appar. Technol. Manag.* **2002**, *2*, 1–12.
13. Islam, R.; Khair, N.; Ahmed, D.; Shahariar, H. Fabrication of low cost and scalable carbon-based conductive ink for E-textile applications. *Mater. Today Commun.* **2019**, *19*, 32–38. [[CrossRef](#)]
14. Zhao, M.; Zhang, Q.; Huang, J.; Tian, G.; Chen, T.; Qian, W.; Wei, F. Towards high purity graphene/single-walled carbon nanotube hybrids with improved electrochemical capacitive performance. *Carbon* **2013**, *54*, 403–411. [[CrossRef](#)]
15. Zhang, X.; Coleman, A.; Katsonis, N.; Browne, W.; Van Wees, B.; Feringa, B. Dispersion of graphene in ethanol using a simple solvent exchange method. *Chem. Commun.* **2010**, *46*, 7539–7541. [[CrossRef](#)]
16. Lux, F. Models proposed to explain the electrical conductivity of mixtures made of conductive and insulating materials. *J. Mater. Sci.* **1993**, *28*, 285–301. [[CrossRef](#)]
17. Tadesse, M.; Mengistie, D.; Chen, Y.; Wang, L.; Loghin, C.; Nierstrasz, V. Electrically conductive highly elastic polyamide/lycra fabric treated with PEDOT: PSS and polyurethane. *J. Mater. Sci.* **2019**, *54*, 9591–9602. [[CrossRef](#)]
18. Zhou, C.E.; Kan, C.W.; Matinlinna, J.P.; Tsoi, J.K.H. Regenerable antibacterial cotton fabric by plasma treatment with dimethylhydantoin: Antibacterial activity against *S. aureus*. *Coatings* **2017**, *7*, 11. [[CrossRef](#)]
19. Ahmad, I.; Kan, C.W. Visible-light-driven, dye-sensitized TiO₂ photo-catalyst for self-cleaning cotton fabrics. *Coatings* **2017**, *7*, 192. [[CrossRef](#)]
20. Saleemi, S.; Naveed, T.; Riaz, T.; Memon, H.; Awan, J.A.; Siyal, M.I.; Xu, F.; Bae, J. Surface functionalization of cotton and PC fabrics using SiO₂ and ZnO nanoparticles for durable flame retardant properties. *Coatings* **2020**, *10*, 124. [[CrossRef](#)]
21. Astm, D. 84 Standard Test Method for Chemical Analysis of Wood Charcoal. *ASTM Int.* **1762**, *84*, 1–2.
22. Hong, J.H.; Pan, Z.J.; Yao, M.; Chen, J.G.; Zhang, Y.X. A large-strain weft-knitted sensor fabricated by conductive UHMWPE/PANI composite yarns. *Sens. Actuator A Phys.* **2016**, *238*, 307–316. [[CrossRef](#)]
23. Batoo, K.M.; Badawi, N.M.; Adil, S.F. Highly sensitive coated cotton thread for applications in the soft circuit. *J. Mater. Sci. Mater. Electron.* **2021**, *32*, 10880–10889. [[CrossRef](#)]
24. ASTM-E1534-93; Standard Test Method for Determination of Ash Content of Particulate Wood Fuels. ASTM International: West Conshohocken, PA, USA, 2013.
25. ASTM E872-82; Standard Test Method for Volatile Matter in the Analysis of Particulate Wood Fuels. Annual Book of ASTM Standard. American Society for Testing and Materials: West Conshohocken, PA, USA, 2013.
26. ASTM D1102-84; Standard Test Method for Ash in Wood. ASTM International: West Conshohocken, PA, USA, 2013.
27. Molina, J. Graphene-based fabrics and their applications: A review. *RSC Adv.* **2016**, *6*, 68261–68291. [[CrossRef](#)]
28. Bashir, S.; Teo, Y.Y.; Ramesh, S.; Ramesh, K.; Mushtaq, M.W. Rheological behavior of biodegradable N-succinyl chitosan-g-poly (acrylic acid) hydrogels and their applications as drug carrier and in vitro theophylline release. *Int. J. Biol. Macromol.* **2018**, *117*, 454–466. [[CrossRef](#)] [[PubMed](#)]
29. Moniha, V.; Alagar, M.; Selvasekarapandian, S.; Sundaresan, B.; Boopathi, G. Conductive bio-polymer electrolyte iota-carrageenan with ammonium nitrate for application in electrochemical devices. *J. Non-Cryst. Solids* **2018**, *481*, 424–434. [[CrossRef](#)]
30. Rivnay, J.; Inal, S.; Collins, B.A.; Sessolo, M.; Stavrinidou, E.; Strakosas, X.; Tassone, C.; Delongchamp, D.M.; Malliaras, G.G. Structural control of mixed ionic and electronic transport in conducting polymers. *Nat. Commun.* **2016**, *7*, 11287. [[CrossRef](#)]
31. Kayser, L.V.; Lipomi, D.J. Stretchable conductive polymers and composites based on PEDOT and PEDOT: PSS. *Adv. Mater.* **2019**, *31*, 1806133. [[CrossRef](#)]
32. Wang, J.; Chen, G.; Wang, S.S. Na-ion conducting gel polymer membrane for flexible supercapacitor application. *Electrochim. Acta* **2020**, *330*, 135322. [[CrossRef](#)]
33. Ahmad, A.; Isa, K.M.; Osman, Z. Conductivity and structural studies of plasticized polyacrylonitrile (PAN)-lithium triflate polymer electrolyte films. *Sains Malays.* **2011**, *40*, 691–694.
34. Furuya, N.; Mineo, N. Preparation of a Concentrated Carbon Black-PTFE Dispersion for Micro-Porous Layer of PEMFC. 2006. Available online: <https://www.semanticscholar.org/paper/Preparation-of-a-Concentrated-Carbon-Black-PTFE-for-Furuya-Mineo/3c477cf4493a7b1320b2dde0a25dee2e4e54c158> (accessed on 27 September 2021).
35. Åkerfeldt, M.; Strååt, M.; Walkenström, P. Electrically conductive textile coating with a PEDOT-PSS dispersion and a polyurethane binder. *Text. Res. J.* **2013**, *83*, 618–627. [[CrossRef](#)]
36. Tseghai, G.B.; Malengier, B.; Fante, K.A.; Nigusse, A.B.; Langenhove, L.V. Development of a flex and stretchy conductive cotton fabric via flat screen printing of PEDOT: PSS/PDMS conductive polymer composite. *Sensors* **2020**, *20*, 1742. [[CrossRef](#)] [[PubMed](#)]
37. Zeng, J.; Dong, L.; Sha, W.; Wei, L.; Guo, X. Highly stretchable, compressible and arbitrarily deformable all-hydrogel soft supercapacitors. *Chem. Eng. J.* **2020**, *383*, 123098. [[CrossRef](#)]
38. Grijalvo, S.; Eritja, R.; Díaz, D.D. On the race for more stretchable and tough hydrogels. *Gels* **2019**, *5*, 24. [[CrossRef](#)]
39. Bonaldi, R.; Siores, E.; Shah, T. Electromagnetic shielding characterisation of several conductive fabrics for medical applications. *Carbon* **2010**, *2*, 237–245. [[CrossRef](#)]
40. Bashir, S.; Hina, M.; Iqbal, J.; Rajpar, A.H.; Mujtaba, M.A.; Alghamdi, N.A.; Wageh, S.; Ramesh, K.; Ramesh, S. Fundamental concepts of hydrogels: Synthesis, properties, and their applications. *Polymers* **2020**, *12*, 2702. [[CrossRef](#)]

41. Atalie, D.; Tesema, A.F.; Rotich, G.K. Effect of weft yarn twist level on thermal comfort of 100 percent cotton woven fabrics. *Res. J. Text. Appar.* **2018**, *22*, 180–194. [[CrossRef](#)]
42. Zhao, L.Z.; Zhou, C.H.; Wang, J.; Tong, D.S.; Yu, W.H.; Wang, H. Recent advances in clay mineral-containing nanocomposite hydrogels. *Soft Matter* **2015**, *11*, 9229–9246. [[CrossRef](#)]
43. Zahid, M.; Papadopoulou, E.; Athanassiou, A.; Bayer, I.S. Strain-responsive mercerized conductive cotton fabrics based on PEDOT:PSS/graphene. *Mater. Des.* **2017**, *135*, 213–222. [[CrossRef](#)]
44. Gong, F.; Meng, C.; He, J.; Dong, X. Fabrication of highly conductive and multifunctional polyester fabrics by spray-coating with PEDOT:PSS solutions. *Prog. Organ. Coat.* **2018**, *121*, 89–96. [[CrossRef](#)]
45. Alamer, F.A. A simple method for fabricating highly electrically conductive cotton fabric without metals or nanoparticles, using PEDOT:PSS. *J. Alloy. Comp.* **2017**, *702*, 266–273. [[CrossRef](#)]
46. Alshammari, A.S.; Shkunov, M.; Silva, S.R.P. Correlation between wetting properties and electrical performance of solution processed PEDOT:PSS/CNT nano-composite thin films. *Coll. Polym. Sci.* **2014**, *292*, 661–668. [[CrossRef](#)]
47. Kim, B.J.; Han, S.H.; Park, J.S. Sheet resistance, transmittance, and chromatic property of CNTs coated with PEDOT:PSS films for transparent electrodes of touch screen panels. *Thin Sol. Film.* **2014**, *572*, 68–72. [[CrossRef](#)]
48. Zhang, J.; Gao, L.; Sun, J.; Liu, Y.; Wang, Y.; Wang, J. Incorporation of single-walled carbon nanotubes with PEDOT/PSS in DMSO for the production of transparent conducting films. *Diam. Relat. Mater.* **2012**, *22*, 82–87. [[CrossRef](#)]

Disclaimer/Publisher’s Note: The statements, opinions and data contained in all publications are solely those of the individual author(s) and contributor(s) and not of MDPI and/or the editor(s). MDPI and/or the editor(s) disclaim responsibility for any injury to people or property resulting from any ideas, methods, instructions or products referred to in the content.